IEEE Access
Multidisciplinary | Rapid Review | Open Access Journal

Received March 28, 2018, accepted May 15, 2018, date of publication May 22, 2018, date of current version June 20, 2018.

Digital Object Identifier 10.1109/ACCESS.2018.2839688

A Comparative Study on Radar Interferometry for Vibrations Monitoring on Different Types of Bridges

ZELONG SHAO[1,2], XIANGKUN ZHANG[1,2], YINGSONG LI[1,3], (Member, IEEE), AND JINGSHAN JIANG[1]

[1]Key Laboratory of Microwave Remote Sensing, National Space Science Center, Chinese Academy of Sciences, Beijing 100190, China
[2]School of Electronic, Electrical and Communication Engineering, University of Chinese Academy of Sciences, Beijing 100049, China
[3]College of Information and Communication Engineering, Harbin Engineering University, Harbin 150001, China

Corresponding author: Xiangkun Zhang (zhangxiangkun@mirslab.cn)

This work was supported in part by the Beijing Natural Science Foundation under Grant 4182077, in part by the National Key Research and Development Program of China under Grant 2016YFE0111100, in part by the Science and Technology Innovative Talents Foundation of Harbin under Grant 2016RAXXJ044, in part by the Key Research and Development Program of Heilongjiang under Grant GX17A016, and in part by the China Postdoctoral Science Foundation under Grant 2017M620918.

ABSTRACT A great number of bridges have been built in the world, which are very important for economic and society developments. Thus, the bridge monitoring is vital and is also a hot topic in recent years. Many bridge monitoring methods have been presented to monitor the bridge vibration. For example, some bridge monitoring methods require the sensors directly contact with the bridge, which might be difficult to install and maintain. In addition, some remote monitoring instruments are expensive and sensitive to the environment. In this paper, a bridge monitoring radar with a central frequency of 36.05 GHz is devised based on a millimeter-wave technology to measure the bridge vibration. It has a super-range resolution of 0.5 m and a high deformation measure precision of 56 μm. Experiments on a high-speed railway bridge and a large cable suspended bridge are performed to verify the effectiveness of the radar interferometry for accurate and precise monitoring of the vibration types and magnitudes of these bridges.

INDEX TERMS Interferometry, millimeter wave radar, remote monitoring, vibration measurement.

I. INTRODUCTION

Bridges are an important part of modern land transportation system. For example, seventy percent of the high-speed railways are bridges in China [1], [2]. Unfortunately, bridge health status would inevitably deteriorate by traffic and environment changes [3], [4]. In addition, accidents and wind will damage the bridges. Thus, bridge status should be carefully monitored in real-time, so that potential issues of bridges could be addressed in time. As a result, sensors such as gauges, accelerometers, total stations, digital levels, global positioning systems (GPS), and interferometry have been studied and used for bridge micro-deformation monitoring [5]–[7]. Each technology has its pros and cons. Devices such as gauges and accelerometers need to be directly installed on the bridges. However, it is dangerous and time-consuming to install them [8]–[10], and it is not allowed to attach anything to the bridge in some cases such as high speed train bridges. Moreover, the installation of these sensors may affect normal operation of traffic and economy. Some non-contact instruments have been used in practice such as GPS, total station, and vision-based systems. However, they are sensitive to the environment. For example, their precision may be degraded during bad weather. Sometimes, these systems would not work in raining or smoggy weather. Radar interferometry can avoid these disadvantages, and therefore had been used in bridge monitoring, civil structure monitoring, and earth mapping [11], [12]. Researchers in Italy have used IBIS system in many bridge monitoring experiments [13], [14]. However, the monitored bridges are simple in structure and there is no comparison between monitoring results obtained from different bridges based on the radar interferometry.

In this paper, various bridges are studied and monitored to verify the effectiveness of the millimeter-wave (mm-wave) radar. The study includes a high-speed railway bridge and the Puli Bridge, which is a large cable-suspended

highway bridge. Experiment results prove that the mm-wave radar system is effective, and can be used for different types of bridge monitoring with high accuracy and precision.

The rest of this paper is organized as follows. The radar measurement principle and the radar architecture are briefly reviewed in Section II. Section III introduces the experiment setup and describes the results obtained by the designed radar. Section IV presents the analysis of different bridge vibrations. In Section V, a concise summary is given.

II. RADAR OPERATING PRINCIPLE AND SYSTEM DESIGN

A. MEASUREMENT PRINCIPLE

To reduce the weight of the radar system, frequency modulated continuous wave (FMCW) mode is used for the radar, which has been introduced in [15] and [16]. Based on the FMCW technique, the radar system avoids the bulky transmitter required in conventional radar. Furthermore, it also reduces the required power of amplifiers. Thus, the devised FMCW radar which is only 2.5 Kg, can meet the requirement of light weight for bridge monitoring. Because bridges' tiny vibration is smaller than 1mm before the structural disaster occured, a high resolution monitoring ability of the radar is required for disaster alarming. For the FMCW radar, the range resolution is limited by frequency bandwidth B of the transmitted signal [17], [18], which is given by:

$$\Delta r = \frac{c}{2B} \tag{1}$$

where c represents the speed of light in vacuum.

If the interferometric technique is not considered in radar system, the minimum position change of a target in range direction measured by the radar will be 0.5m with a bandwidth of 300MHz. When the interferometric technique is considered, the micro-deformation detection ability of the radar can be improved in the range direction. In this circumstance, the minimum deformation measured by the radar is affected by the phase difference of echoes at different times [19], [20]. The relationship between the deformation of the objective and the phase difference of echoes from different observations can be described by:

$$\Delta R = \frac{\lambda}{4\pi}\Delta\varphi \tag{2}$$

where ΔR is the position changes of the bridge on the line of sight, $\Delta\varphi$ is the phase shift between echoes at different observations, λ is the wave-length of the electromagnetic wave in its central frequency. Since λ is small at mm-wave signal, the minimum position changes of the target which can be measured by the radar is small too. Moreover, the precision of the measured deformation is affected by the phase precision of the reflected wave. To get an accurate phase changes when the position of target is changed, phase unwrapping and phase calibrated methods have been used in the previous articles [21], [22].

When the radar is used for monitoring a bridge, the measured deformation on the line of sight is not equal to the real deformation of the bridge. Herein, the viewing geometric structure of the bridge monitoring is considered and used for calculating the real deformation. It is given in Fig. 1.

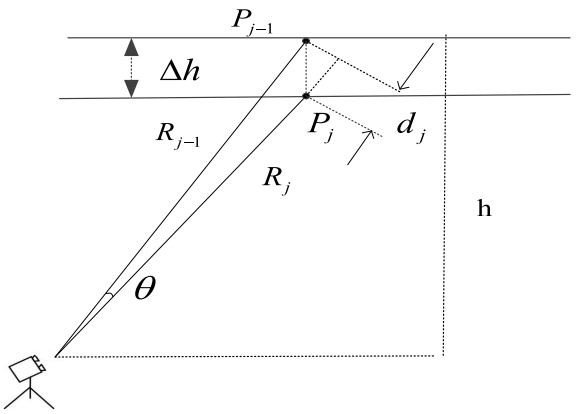

FIGURE 1. Diagram of displacement correction scheme.

From Fig.1, the deformation on the direction of sight can be expressed as

$$d_j = R_{j-1} - R_j \quad (j = 1, 2, 3 \cdot \cdot) \tag{3}$$

If the angle is small, we have

$$\Delta h^2 = d_j^2 + (R_{j-1}\theta)^2 - 2R_{j-1}\theta \cdot d_j \cdot \cos(\frac{\pi - \theta}{2}) \tag{4}$$

where

$$(R_{j-1}\theta) - 2 \cdot d_j \cdot \sin(\frac{\theta}{2}) \approx (R_{j-1} - d_j)\theta \tag{5}$$

Thus, we have

$$\Delta h = \sqrt{d_j^2 + (R_{j-1}\theta)^2(R_{j-1} - d_j)} \tag{6}$$

Usually, the distance between the radar and target is much greater than the deformation on the direction of sight, which means that the deformation on the direction of sight is very small and is difficult to measure in practical engineering. To accurately measure the micro-deformations, many experiments of measuring a moving corner reflector's position on the slide rail have been performed by our team to verify the micro-deformation measure ability of the radar [23]. Experiments proved that the devised radar has a high precision in the target's position changes measure ability, which is as little as 56 μm. Compared with other target position measure instruments, it has a higher precision. Comparisions between different deformation measure technologies are shown in Table 1.

TABLE 1. Comparison of different deformation measure technologies.

Type	Proposed Radar	GPS	Total Station	Deflectometer
Precision	sub-mm	5 mm	2mm	0.1 mm

In fact, the micro-deformation measurement results are calculated by using the above equation (6). Thus, the micro-deformation obtained by the radar system will be affected by

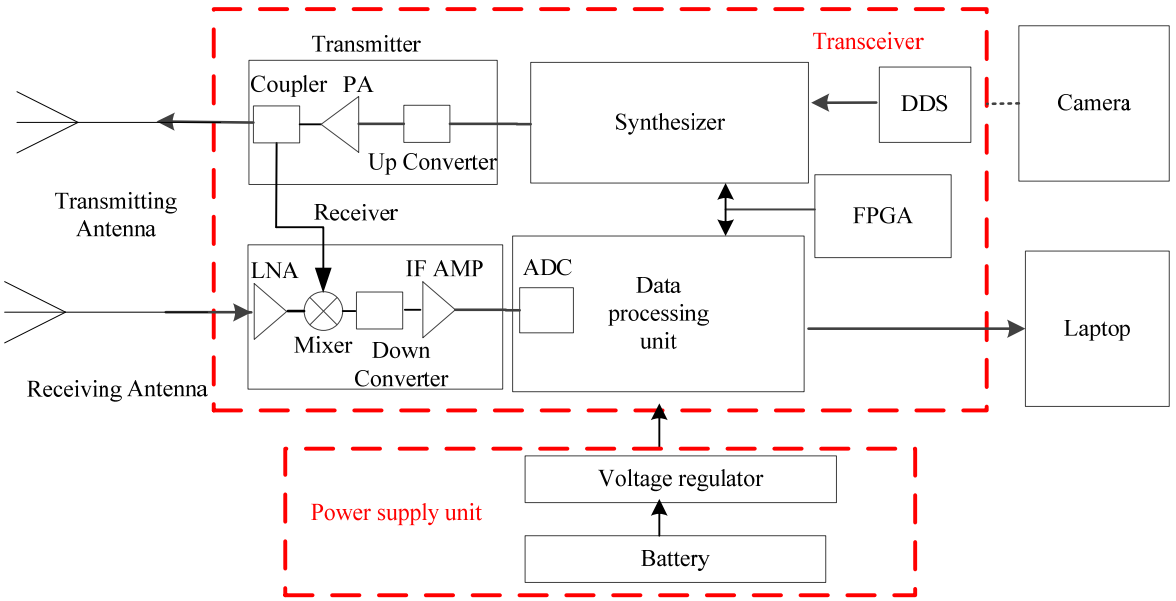

FIGURE 2. Block diagram of the mm-wave radar.

the radar's position and angle of elevation. Since the bridge's vibration is usually weak, the radar is placed on stable foundation under the bridge. If the bridge is long enough, it would be better to install the radar on the place where its antennas are vertically pointed to the underneath of the bridge. In addition, it can also be installed on one side of the bridge with an elevation angle not smaller than 30°.

B. RADAR STRUCTURE

The designed mm-wave radar consists of antennas, transmitter, receiver, data processing module, and power supplies. Slot array antennas are used for transmitting and receiving signals separately. In the data processing module, a controller unit and a signal sampling unit are used for time sequence control and data processing. For the transceiver module, radio frequency signals are generated and received at the same time. Mixing the received signal with a local replica of the transmitting signal maintains coherence and makes the system compact. The detailed diagram of the proposed mm-wave radar is illustrated in Fig. 2.

Two waveguide slot arrays antennas scheme for transmitting and receiving respectively is to solve the isolation problem. The isolation between the transmitting and receiving antennas is 60 dB to guarantee the transmitting and receiving signals with a very low mutual coupling, which can improve the dynamic range of the radar. Each antenna has a beam width of $4° \times 10°$, which can make the electromagnetic wave oriented to the measure target, avoiding noise in the environment. For example, the illuminated area in the large cable suspended bridge monitoring experiment is only 12.8 m in width. It is smaller than the bridge width (24 m). Thus, the echo acquired by the antennas is pure without too much noise. The antennas are connected with the transmitter and receiver module with a rectangular waveguide to coaxial-line transducer. Additionally, the antennas are fabricated with 4 sub-layers, namely, slot layer, flange layer, waveguide layer and the feed network.

In the transmitter, a linear frequency-modulated chirp signal with 300MHz bandwidth is generated by a direct digital synthesizer DDS and then modulated to 3750MHz $\pm$150 MHz intermediate frequency (IF). This IF chirp signal is sent to the mm-wave transmitter and up-converted to radio frequency (RF) signal with a center frequency of 36.05 GHz for transmitting. In comparison with the transmitter, the receiver consists of a low noise amplifier (LNA), a mixer and an IF amplifier. The LNA amplifies the weak echo signal. The amplified signal is down-converted to IF. The IF amplifier further boosts the IF signal and sends it to a 16-bit ADC with 10MHz sampling rate, which converts the IF signal into digital data. A high-speed compact flash (CF) card is used to store the data. An FPGA processing unit is used as the controller for the radar system [24].

For convenience in field test, power supply unit of the radar includes a battery and a voltage regulator. As a synchronous surveying instrument, a camera is applied to get optical image of the objective. The designed radar is shown in Fig.3. Its parameters are listed in Table 2.

To provide a user-friendly interface and achieve real time processing, a laptop is used to handle the measured data. A bridge monitoring software named "Radar interferometry for bridge monitoring" is used for data visualization and analysis. The graphic user interface (GUI) of the software is shown in Fig.4, including the vibration analysis in both time domain and frequency domain.

Furthermore, specific parameters of the bridge monitoring experiments can be imported into the software to make signal

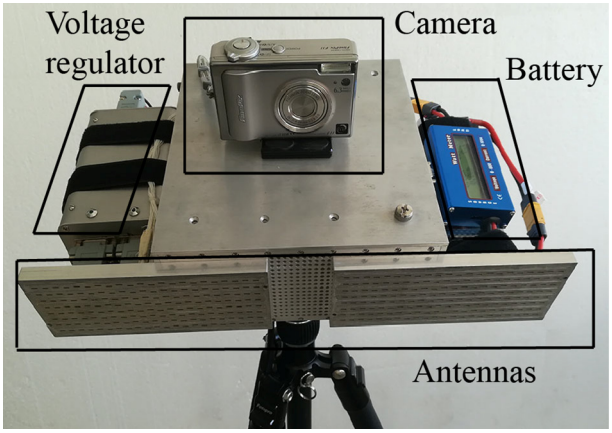

FIGURE 3. The photo of mm-wave radar.

TABLE 2. Parameters of the radar.

Parameter	Value	Paremeter	Value
Bandwidth	300 MHz	Sidelobe Suppresion	>18dB
Central Frequency	36.05 GHz	VSWR	<2
Transmitted Power	23dBm	Impedance	50Ω
Antenna Gain	30dB	Max. Power	50W
EIRP	50dBm	Beam Angle	4°×10°

Note: EIRP-Effective Isotropic Radiated Power; VSWR- Voltage Standing Wave Ratio;

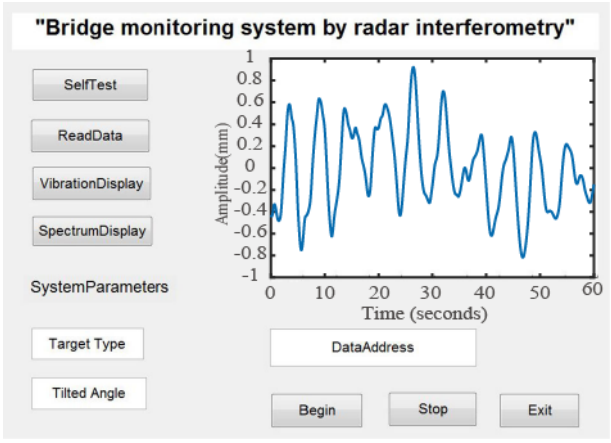

FIGURE 4. Software interface.

process flexible. For example, the slant angle can be specified and other parameters can also be imported, such as the target type, data address.

To verify the effectiveness and the stability of the radar, various experiments have been performed, which will be discussed in the next section.

III. EXPERIMENTS

A. MONITORING EXPERIMENT OF HIGH-SPEED RAILWAY BRIDGE

On the basis of the previous experiments, the train on the light rail which runs slower than the high-speed rail has been measured by the designed mm-wave radar system [25]. Herein, the proposed mm-wave radar system is used to measure the vibration of a high-speed railway bridge to broaden its application regions. A bridge of Beijing-Tianjin high-speed railway which is near the sixth ring road of Beijing is investigated in the paper. Here, the speed of the train can reach up to 350km/h. The setup of this experiment is shown in Fig.5.

FIGURE 5. Experiment setup of the highs-peed railway bridge.

The vibration of the bridge is obtained when two trains are passing through the bridge in opposite direction, and the monitoring result obtained by the designed mm-wave radar is presented in Fig.6. From Fig.6, it can be seen that the bridge is static if there is no train running on the bridge. The status of the bridge changes quickly when the train is passing through the railway. Thus, high-speed moving trains strike the railway to produce strong vibration during the time periods from 2 to 5 seconds and from 11 to 14 seconds. The residual vibration in the time periods from 5 to 9 seconds is larger than the residual vibration during the time periods from 14 to 18 seconds. This may be caused by the position of the radar system because the radar system is set under the right

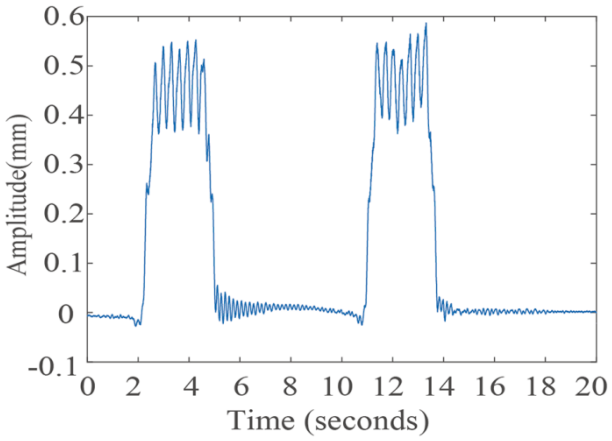

FIGURE 6. Experiment result on vertical vibration of the high-speed railway bridge.

side of the bridge. Thus, the vibration caused by the train running on the right side of the railway is stronger than that of the left side. Namely, the train which runs from south to north causes a stronger bridge vibration.

The spectrum of the bridge vibration can be gotten, which is descripted in Fig.7. It is found that the vibration of the bridge during the measurement time is comprised of a low frequency vibration which is about 3.2Hz and a high frequency vibration which is about 6.2Hz.

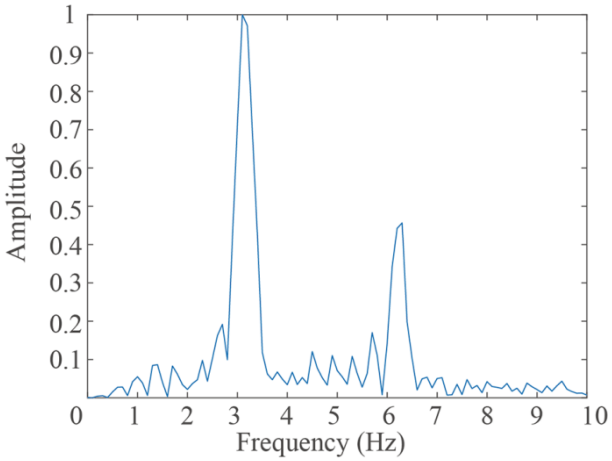

FIGURE 7. Spectrum of the vertical vibration of the high-speed railway bridge.

To distinguish the two frequencies, bridge vibrations in different time periods are analyzed in detail. In this paper, we analyze the bridge vibration in three different time periods, namely from 2 to 5 seconds, from 5 to 10 seconds, and from 11 to 14 seconds. The spectrum of the bridge vibration from 2 to 5 seconds is the same with the spectrum of the bridge vibration from 11 to 14 seconds, because two different trains pass through the bridge during the two time periods respectively. Thus, spectrums in two time periods are shown in the paper, namely from 2 to 5 seconds and from 5 to 10 seconds. The corresponding spectrums of the vibration in these two different time periods are shown in Fig. 8 and Fig.9, respectively. From the above analysis, the loading frequency vibration of the bridge is mostly found in the time periods from 2 to 5 seconds and from 11 to 14 seconds when there is a train on the bridge [26]. Whereas, the natural frequency vibration of the bridge is located in the time periods from 5 to10 seconds when the residual vibration occurs.

The bridge is a prestressed continuous concrete bridge which has many spans. It is supported by many simple supported box girders that are 32 meters in length, 11 meters in height and 10 meters in width. In this case, the loading frequency of the bridge's box girder caused by the train is approximately 3Hz, which is related with the length of the cabin of the train. The relationship can be descripted by equation (7). In this experiment, the velocity of the train is about 300km/h and the length of a cabin is 25 meters.

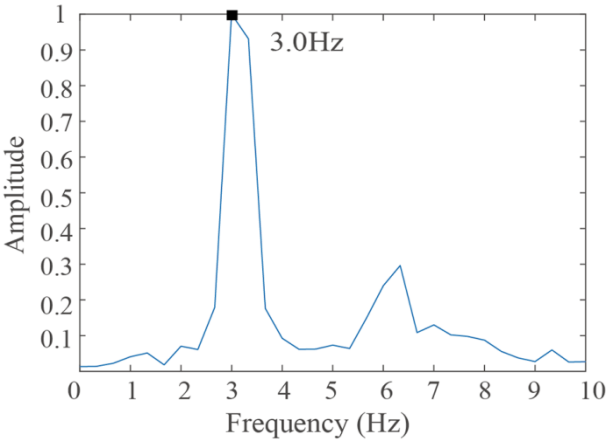

FIGURE 8. Spectrum of the bridge vibration from 2 to 5 seconds.

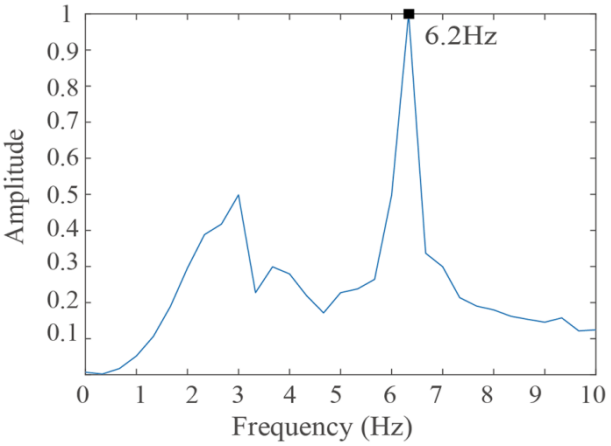

FIGURE 9. Spectrum of the bridge vibration from 5 to 10 seconds.

Thus, the loading frequency (3.0Hz) measured in the experiment is approximately equal to the frequency (3.3Hz) calculated by using equation (7) in theory.

$$f = \frac{v}{L} \tag{7}$$

The natural vibration of the bridge can be affected by the structure and material of the bridge's concrete blocks [27], [28]. It can be depicted by equation (8).

$$f_s = \frac{1}{2\pi}\sqrt{\frac{\frac{1}{2}EI_b\left(\frac{\pi}{L_b}\right)^4 L_b}{\frac{1}{2}m_b L_b}} \tag{8}$$

where EI_b is the stiffness of the vertical bending of the bridge, L_b is the length of bridge span, and m_b is the weight of the bridge per unit length.

In this experiment, the length of the bridge span is 32 meters, and the stiffness is 1219861N/m. Thus, the natural frequency of the bridge's vibration is about 6Hz, which is approximately equal to the vibration frequency of the bridge in the time periods from 5 to 10 seconds.

B. MONITORING EXPERIMENT OF PULI BRIDGE

Bridges with long-span are flexible because they are easily affected by the environment factors. Thus, their vibrations should be monitored and analyzed carefully to avoid disaster or accident [29]. In this paper, Puli Bridge, which is a large cable-suspended bridge, is monitored by the designed mm-wave radar. As we know, Puli Bridge is the first highway bridge in mountainous areas in the southwestern China. It is a typical cable-suspended bridge which crosses the Puli canyon whose depth is about 400 meters. The appearance and structure of the Puli Bridge are shown in Fig.10(a).

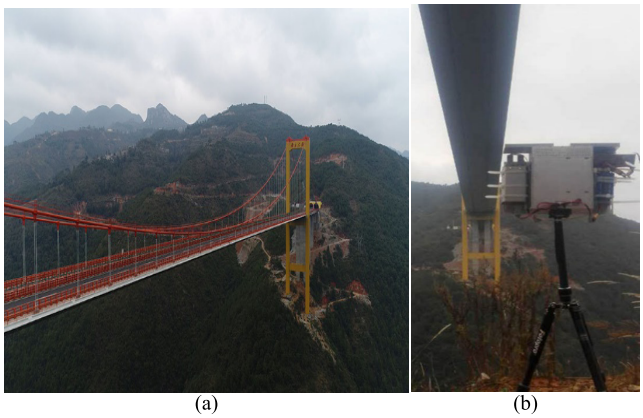

FIGURE 10. Test scenario of Puli Bridge. (a) Bridge appereance. (b) Experiment setup.

The bridge is comprised of a central span of 628 meters and two lateral spans of 166 meters. The deck of the bridge is suspended by two cables which are arranged at each side of the bridge. Additionally, the two main cables are connected to two H-shaped reinforced concrete towers whose height is about 160 meters from the foundations [30]. To measure the bridge vibration, the radar system is installed under the Puli Bridge, which is set on the earth. The experiment setup is shown in the Fig.10(b).

Since the deformation of the bridge can be obtained from the phase of the reflected signal, the vertical vibration of Puli Bridge gotten by the radar measurement is presented in Fig.11 and Fig.13 when there is a vechile passes through the bridge or not. Obviously, the amplitude is less than 1 mm during the entire measurement periods when there is no vehicle passing the monitored region of the bridge.The spectrum of the vibration is illustrated in Fig. 12. It can be seen that the bridge's vibration is consistent with frequencies acquired in the research by the simulation tool ANSYS [31].

Compared the experiment results with the simulation results in Table 3 analyzed by ANSYS, we can see that the natural vibration frequencies of the bridge are nearly same with that of the simulation results which are identified by using the asterisk. From the Table 3, it is obvious that the main frequency of the bridge vibration acquired by the radar is caused by the vertical bending of the significant girder.

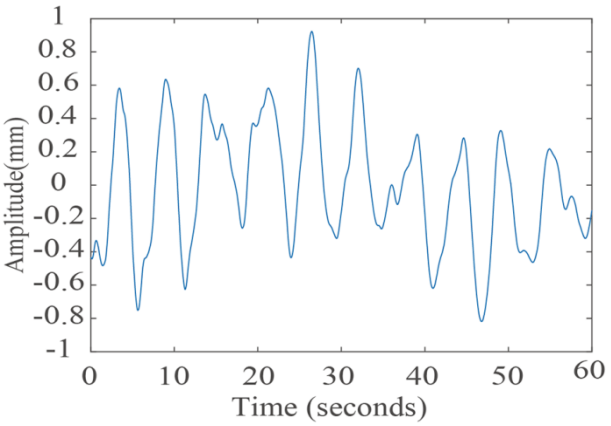

FIGURE 11. Bridge vibration when there was no vehicle.

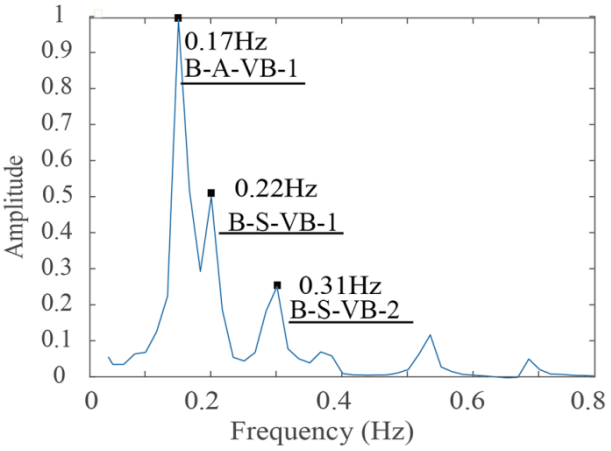

FIGURE 12. Spectrum of the bridge vibration when there was no vehicle.

TABLE 3. Comparison of Results by the radar and by ANSYS.

Model	Frequency /Hz	Type	Fig.12	Fig.14
1	0.121	B-A-VB+ M-1		
2	0.37	B-S-TB-1		
3	0.174	B-A-VB-1	*	*
4	0.226	B-S-VB-1	*	
5	0.306	B-S-VB-2	*	
6	0.394	B-A-VB -2		*

Note: B-main beam; S-symmetry; A-opposition; VB-vertical bending; TB-horizontal bending; T-twist; M-drift;

Similarly, the bridge vibration is depicted in Fig.13 when a vehicle passes through the monitored region of the bridge. Obviously, the amplitude is very large during the time periods from 30 to 50 seconds, which is caused by the strike of the vehicle on the bridge.

The spectrum of the vibration is presented in Fig. 14. The experiment result is consistent with the simulation result in Table 3 except the smallest frequency of the bridge's

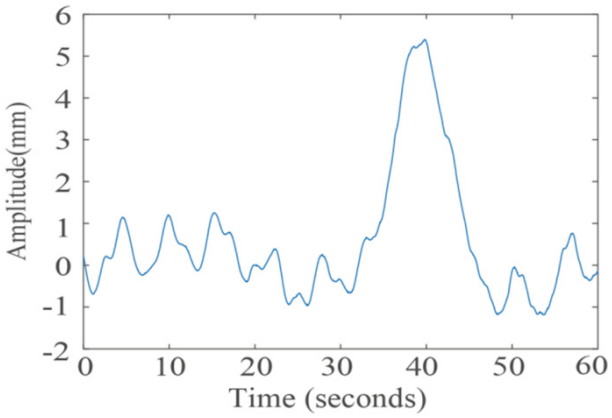

FIGURE 13. Bridge vibration when there was a vehicle.

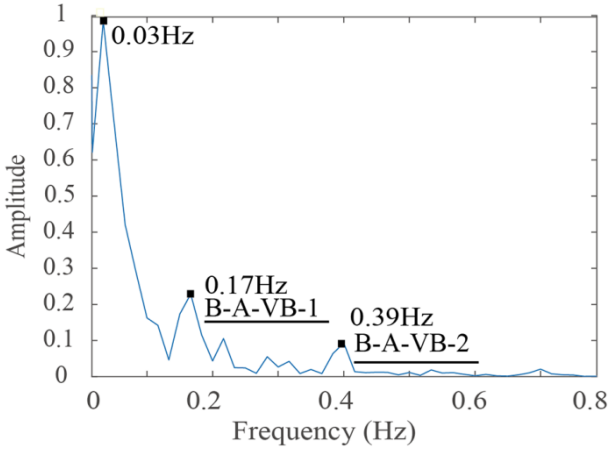

FIGURE 14. Spectrum of the bridge vibration when there was a vehicle.

vibration (0.03Hz). It is not the natural vibration of the bridge and is caused by the strike of the vehicle passing by the bridge.

The frequency of the bridge vibration caused by the vehicle can be calculated by the above equation (7). In the experiment, the vehicle is a truck whose velocity is about 100km/h. And, the length of the bridge is about 960 meters. Thus, the loading vibration frequency is about 0.03Hz.

IV. DISCUSSION

From the experiment result of the high-speed railway bridge vibration monitoring, it is obvious that that the calculation method for loading vibration is similar with the calculation method for loading vibration of the light-railway bridge. In addition, the calculation method for the natural vibration of the high-speed railway bridges has been proposed in this paper.

For the monitoring of Puli Bridge, the radar measurement results have been compared with the ANSYS simulations. It can be concluded that the main frequencies of the bridge vibration are caused by the bending and twisting of the main girder. Meanwhile, the vibration of Puli Bridge is complex because of its structure, material and geographical position. For example, it is easy to vibrate because it lies in the mountainous areas where there is a harsh environment. Namely, there may have strong wind, heavy rain and heavy fog usually. Thus, it is necessary and important to monitor the status of such bridges.

In addition, we found that the loading vibration generated by the vehicles on the bridge is consistent with the loading vibration of high speed railway bridges analyzed above. The loading vibration frequency can be also calculated by equation (7). From the comparison between the experiment and the ANSYS analysis, we can see that the dominate vibration frequency caused by the main grider of the bridge comes from the opposite symmetry vertical bending vibration and symmetry vertical bending vibration. Overall, we can conclude that the mm-wave radar has the ability of measure the vibrations of large cable-suspended bridges accurately.

V. CONCLUSION

A mm-wave radar is designed based on interferometry technology and used for bridge deformation monitoring applications. The designed radar is used to accurately measure the bridge vibration. Experiments prove that the mm-wave radar can be used for monitoring different types of bridges such as light railway bridges in city, high-speed railway bridges in countryside and large cable-suspended bridges in mountainous areas. Thus, the mm-wave radar system has a bright application prospective in the future for its high measure performance such as micro-deformation measure ability in submillimeter level and advanced structural characteristics such as portable with a weight of 2.5 Kg.

REFERENCES

[1] X. He *et al.*, "Recent developments of high-speed railway bridges in China," *Struct. Infrastruct. Eng.*, vol. 13, no. 12, pp. 1584–1595, 2017.
[2] X. He, Z. Yu, and S. Hu, "Main achievements and technical challenges of high-speed railway bridges in China," in *Proc. IABSE Conf.*, 2016, pp. 820–826.
[3] Z. X. Li, T. H. T. Chan, and J. M. Ko, "Evaluation of typhoon induced fatigue damage for Tsing Ma Bridge," *Eng. Structures*, vol. 24, no. 8, pp. 1035–1047,2002.
[4] D. Marzougui, S. Jin, and R. A. Livingston, "Development of an LS-DYNA nonlinear finite element model for use in damage detection and health monitoring of highway bridges," *Proc. SPIE*, vol. 4337, pp. 432–440, Aug. 2001.
[5] M. R. Chowdhury and J. C. Ray, "Accelerometers for bridge load testing," *NDT & E Int.*, vol. 36, no. 4, pp. 237–244, 2003.
[6] X. Yu and H. Xue, "Method of bridge vibration monitoring based on GPS and accelerometer," (in Chinese), *J. Southeast Univ., Nat. Sci. Ed.*, vol. 43, no. 2, pp. 329–333, 2013.
[7] Z. Zhang and Q. Liu, "Research of bridge health monitoring data acquisition system," *Boletín Técnico*, vol. 55, no. 10, pp. 411–418, 2017.
[8] C. Gentile, "Application of microwave remote sensing to dynamic testing of stay-cables," *Remote Sens.*, vol. 2, no. 1, pp. 36–51, 2010.
[9] G. Luzi, M. Crosetto, and E. Fernández, "Radar interferometry for monitoring the vibration characteristics of buildings and civil structures: Recent case studies in Spain," *Sensors*, vol. 17, no. 4, p. 669, 2017.
[10] C. Li, W. Chen, G. Liu, R. Yan, H. Xu, and Y. Qi, "A noncontact FMCW radar sensor for displacement measurement in structural health monitoring," *Sensors*, vol. 15, no. 4, pp. 7412–7433, 2015.
[11] M. Pieraccini, F. Parrini, M. Fratini, C. Atzeni, P. Spinelli, and M. Micheloni, "Static and dynamic testing of bridges through microwave interferometry," *NDT & E Int.*, vol. 40, no. 3, pp. 208–214, 2007.

[12] C. Gentile and G. Luzi, "Radar-based dynamic testing of the cable-suspended bridge crossing the Ebro River at Amposta, Spain," in *Proc. 11th Int. VMLC*, 2014, p. 180.
[13] M. Pieraccini, M. Fratini, F. Parrini, G. Macaluso, and C. Atzeni, "High-speed CW step-frequency coherent radar for dynamic monitoring of civil engineering structures," *Electron. Lett.*, vol. 40, no. 14, pp. 907–908, Jul. 2004.
[14] S. Hensley, D. Moller, S. Oveisgharan, T. Michel, and X. Wu, "Ka-band mapping and measurements of interferometric penetration of the Greenland ice sheets by the GLISTIN radar," *IEEE J. Sel. Topics Appl. Earth Observ. Remote Sens.*, vol. 9, no. 6, pp. 2436–2450, Jun. 2016.
[15] M. Edrich, "Ultra-lightweight synthetic aperture radar based on a 35 GHz FMCW sensor concept and online raw data transmission," *IEE Proc.-Radar, Sonar Navigat.*, vol. 153, no. 2, pp. 129–134, Apr. 2006.
[16] H. Wang, M. Jiang, and S. Zheng, "Airborne Ka FMCW MiSAR system and real data processing," in *Proc. 17th Int. Radar Symp.*, 2016, pp. 1–5.
[17] H.-H. Ko, K.-W. Cheng, and H.-J. Su, "Range resolution improvement for FMCW radars," in *Proc. 5th Euro. Radar Conf.*, 2008, pp. 352–355.
[18] C. Wang, H. Zhang, and Z. Liu, *Spaceborne Synthetic Aperture Radar Interferometry*. Beijing, China: Science Press, 2002.
[19] D. Dei, M. Pieraccini, M. Fratini, C. Atzeni, and G. Bartoli, "Detection of vertical bending and torsional movements of a bridge using a coherent radar," *NDT & E Int.*, vol. 42, no. 8, pp. 741–747, 2009.
[20] K. T. Hsu, C. C. Cheng, and C. H. Chiang, "Long-term monitoring of two highway bridges using microwave interferometer-case studies," in *Proc. 16th Int. Conf. (GPR)*, 2016, pp. 1–5.
[21] R. M. Goldstein, H. A. Zebker, and C. L. Werner, "Satellite radar interferometry: Two-dimensional phase unwrapping," *Radio Sci.*, vol. 23, no. 4, pp. 713–720, Aug. 1988.
[22] X. Liu, X. Tong, K. Ding, X. Zhao, L. Zhu, and X. Zhang, "Measurement of long-term periodic and dynamic deflection of the long-span railway bridge using microwave interferometry," *IEEE J. Sel. Topics Appl. Earth Observ. Remote Sens.*, vol. 8, no. 9, pp. 4531–4538, Sep. 2015.
[23] Z. Shao, X. Zhang, and Y. Li, "Analysis and validation of super-resolution micro-deformation monitoring radar," *Prog. Electromagn. Res. M*, vol. 62, no. 12, pp. 41–50, 2017.
[24] M. Y. Chua and V. C. Koo, "FPGA-based chirp generator for high resolution UAV SAR," *Prog. Electromagn. Res.*, vol. 99, no. 4, pp. 71–88, 2009.
[25] X. Zhang, Z. Shao, J. Ren, J. Jiang, and Y. Li, "Performance verification and testing for micro deformation detection radar," in *Proc. PIERS*, 2017, pp. 295–298.
[26] J. Li and M. Su, "The resonant vibration for a simply supported girder bridge under high-speed trains," *J. Sound Vib.*, vol. 224, no. 5, pp. 897–915, 1999.
[27] V. A. L. Chasteau, "The use of tuned vibration absorbers to reduce wind-excited oscillations on a steel footbridge," *Civil Eng. South Africa*, vol. 15, no. 6, pp. 147–154, 1973.
[28] W. Wang, Y. Yang, P. Liu, and J. Yao, "Analysis of influence of MTMD on the vertical vibration character of high-speed railway 32 m prestressed concrete simply supported box beam," (in Chinese), *Environ. Eng.*, vol. 30, no. 1, pp. 153–155, 2012.
[29] C. Gentile and G. Bernardini, "Radar-based measurement of deflections on bridges and large structures," *Eur. J. Environ. Civil Eng.*, vol. 14, no. 4, pp. 495–516, 2010.
[30] G. Huang *et al.*, "Response analysis of long-span suspension bridge under mountainous winds," (in Chinese), *J. Southwest Jiaotong Univ.*, vol. 50, no. 4, pp. 610–616, 2015.
[31] W. Huang, J. Sun, K. Zou, and M. Wang, "Buffeting response analysis of the suspension bridge in time domain," (in Chinese), *J. Xi'an Unie. Archit. Technol., Natural Sci. Ed.*, vol. 47, no. 3, pp. 371–375, 2015.

ZELONG SHAO was born in Linyi, Shandong, China, in 1989. He received the B.S. degree in control technology and instrument from the China University of Geosciences, Wuhan, China, in 2011, and the M.S. degree in control engineering from the University of Chinese Academy of Sciences, Beijing, China, in 2015. Since 2016, he has been studied in the National Space Science Center, Chinese Academy of Sciences, Beijing. His current research interests include microwave remote sensing system design and radar application technology.

XIANGKUN ZHANG was born in Yantai, Shandong, China, in 1972. He received the B.S. degree in electrical engineering from Harbin Engineering University, Harbin, China, in 1994, and the Ph.D. degree in computer application technology from the University of Chinese Academy of Sciences, Beijing, China, in 2007. Since 2002, he has been with the National Space Science Center, Chinese Academy of Sciences, Beijing. His current research interests include microwave remote sensing and imaging theory and radar technology.

YINGSONG LI (M'09) was born in Luoyang, Henan, China, in 1982. He received the B.S. degree in electrical and information engineering and the M.S. degree in electromagnetic field and microwave technology from Harbin Engineering University, China, in 2006 and 2011, respectively, and the Ph.D. degree from the Kochi University of Technology (KUT), Japan, and Harbin Engineering University, in 2014. From 2016 to 2017, he was a Visiting Scholar with the University of California, Davis. Since 2014, he has been a Full Professor with Harbin Engineering University. He is also a Visiting Professor with Far Eastern Federal University and KUT. His current research interests are mainly in underwater communications, signal processing, compressed sensing, and antennas. He is a Senior Member of the Chinese Institute of Electronics. He is an Associate Editor of the IEEE Access and the *AEÜ-International Journal of Electronics and Communications*. He serves as a reviewer for over 20 journals.

JINGSHAN JIANG was born in Longjing, Jilin, China, in 1936. He received the B.S. degree from the Leningrad Urianov Electrical Engineering College, Russia, in 1962. From 1981 to 1983, he was a Visiting Scholar in USA. He is currently a Full Professor with the National Space Science Center, Chinese Academy of Sciences, Beijing, China. His current research interests include microwave remote sensing and radar imaging technology.

He is an Academician of the China Engineering Academy. He is a member of the International Eurasian Academy of Sciences. He is the Vice Chief Design Engineer of the China's Moon Probe Program and an Advisor for the Space Field Committee of 863 Project.